J. Fluid Mech. (1995), *vol.* 305, *pp.* 77–91

Solution breakdown in a family of self-similar nearly inviscid axisymmetric vortices

By R. FERNANDEZ-FERIA[1], J. FERNANDEZ DE LA MORA[2] AND A. BARRERO[3]

[1] Universidad de Málaga, ETS Ingenieros Industriales, 29013 Málaga, Spain

[2] Yale University, Mechanical Engineering Dept., New Haven, CT 06520-2159, USA

[3] Universidad de Sevilla, ETS Ingenieros Industriales, 41012 Sevilla, Spain

(Received 15 March 1995)

Many axisymmetric vortex cores are found to have an external azimuthal velocity v, which diverges with a negative power of the distance r to their axis of symmetry. This singularity can be regularized through a near-axis boundary layer approximation to the Navier–Stokes equations, as first done by Long for the case of a vortex with potential swirl, $v \sim r^{-1}$. The present work considers the more general situation of a family of self-similar inviscid vortices for which $v \sim r^{m-2}$, where m is in the range $0 < m < 2$. This includes Long's vortex for the case $m = 1$. The corresponding solutions also exhibit self-similar structure, and have the interesting property of losing existence when the ratio of the inviscid near-axis swirl to axial velocity (the *swirl parameter*) is either larger (when $1 < m < 2$) or smaller (when $0 < m < 1$) than an m-dependent critical value. This behaviour shows that viscosity plays a key role in the existence or lack of existence of these particular nearly inviscid vortices, and supports the theory proposed by Hall and others on vortex breakdown. Comparison of both the critical swirl parameter and the viscous core structure for the present family of vortices with several experimental results under conditions near the onset of vortex breakdown show a good agreement for values of m slightly larger than 1. These results differ strongly from those in the highly degenerate case $m = 1$.

1. Introduction

Axisymmetric swirling flows at high Reynolds numbers have several distinctive properties, including the phenomenon of vortex breakdown and the fact that swirl and axial jets appear often as inseparable features. These phenomena have been discussed widely, although they remain largely unexplained. For instance, the issue of whether viscosity is or is not an important actor in this play has been discussed for quite some time (e.g. Batchelor 1964), but it remains unsettled, as evident from the fact that vortex breakdown has been interpreted by some as a purely inviscid phenomenon (as in Benjamin's 1962 theory, or in Batchelor's 1967 model and its extension by Buntine & Saffman 1995), and as a fundamentally viscous problem by others (as in Hall's analogy to boundary layer separation, e.g. Hall 1972). Of course, broad fluid mechanical questions such as this can rarely be answered in general, as illustrated for instance by instability problems, governed sometimes, though by no means always, by inviscid criteria. In the present article we consider a simple model problem involving a family of nearly inviscid axisymmetric vortices, for which viscosity definitely plays a key global role.

The flows analysed in this work are exact solutions to the axisymmetric boundary

layer approximation of the Navier–Stokes equations. They match a class of inviscid vortical motions whose axial and azimuthal velocities and pressure vary near the axis as powers of the distance r to the axis:

$$w = lW_0 r^{m-2}, \tag{1}$$

$$v = \pm LW_0 r^{m-2}, \tag{2}$$

$$\frac{p}{\rho} = \frac{(LW_0)^2}{2(m-2)} r^{2(m-2)}, \tag{3}$$

with $0 < m < 2$. In the above expressions, (u, v, w) is the velocity field in polar cylindrical coordinates (r, θ, z). p is the pressure, ρ the fluid density, $l = \pm 1$, and W_0 and L are arbitrary (positive) constants. Although equations (1)–(3) have cylindrical symmetry, they correspond to the near-axis behaviour ($r/z \ll 1$) of a family of conically similar solutions to the incompressible Euler equations (Fernandez-Feria, Fernandez de la Mora & Barrero 1995). The radial velocity u is shown to be zero at the lowest order. The case $m = 1$ corresponds to a potential vortex ($v \sim r^{-1}$), which has been widely considered in the literature (see references given below). However, for both confined and free vortices, the quasi-inviscid flow around viscous vortex cores is found, in general, to be non-potential, with an azimuthal velocity proportional to r^{-n}, where the power n ranges between 0.4 and 1 ($1 < m < 1.6$ in (1)–(3)), depending on the particular physical situation (see e.g. Ogawa 1993 for a review on experimental data of many different types of vortices).

The *swirl parameter*, L, or ratio between azimuthal and axial inviscid velocities near the axis,

$$L \equiv |v/w|_{r/z \to 0}, \tag{4}$$

plays an important role in vortex flows because numerical and experimental results (see e.g. Spall, Gatski & Grosh 1987) show that, for high Reynolds numbers, vortex breakdown occurs when the ratio v/w at the edge of the viscous core of the vortex is larger than a critical value which is near 1.5 (see §5 for details). This parameter also characterizes solution breakdown in the present family of vortices.

The axial and azimuthal velocities (1)–(2) and their derivatives with respect to r are singular at the axis when $0 < m < 2$. Therefore, even at very high Reynolds numbers, it is inconsistent within the framework of the Navier–Stokes equations to ignore viscosity in a certain narrow region near the axis. The structure of the viscous core for a *quasi-free vortex* such as (2) has sometimes been modelled using semi-empirical expressions which behave as a rigid rotation for small r, and match a negative power of radius for large r (see e.g. Vatistas, Kozel & Mih (1991) and Ogawa 1993). Here we shall obtain exact self-similar solutions to the near-axis boundary layer approximation of the Navier–Stokes equations. In contrast to other similarity solutions for viscous vortex cores (e.g. Hall 1961; Stewartson & Hall 1963; Mayer & Powell 1992, among others), ours match with external vortical inviscid flows which are exact solutions to the Euler equations. As mentioned above, a near-axis ($r/z \ll 1$) azimuthal velocity proportional to a power of the radius (equation (2)) models the external inviscid flow observed in many real vortices. The case $m = 1$, where the complete Navier–Stokes equations admit exact conical solutions, has been studied extensively, both with and without swirl (e.g. Landau 1944; Squire 1951, 1952; Goldshtik 1960; Yih *et al.* 1982; Paull & Pillow 1985*a*, *b*; Pillow & Paull 1985; Bojarevics *et al.* 1989; Goldshtik & Shtern 1990; Sozou 1992; Sozou, Wilkinson & Shtern 1994, among others). The boundary layer form of the swirling problem with $m = 1$ and $l = +1$ was first considered by Long (1958, 1961), and has been the subject of numerous subsequent investigations (e.g. Burggraf & Foster

1977; Foster & Duck 1982; Foster & Smith 1989; Foster & Jacqmin 1992; Khorrami & Trivedi 1994; Drazin, Banks & Zaturska 1995).

2. Governing equations

In cylindrical polar coordinates, the near-axis boundary layer approximation to the Navier–Stokes equations (sometimes called *quasi-cylindrical* approximation in the literature on vortex breakdown) for a steady incompressible and axisymmetric flow may be written as

$$\frac{1}{r}\frac{\partial}{\partial r}(ru)+\frac{\partial w}{\partial z}=0, \tag{5}$$

$$\frac{v^2}{r}=\frac{\partial(p/\rho)}{\partial r}, \tag{6}$$

$$u\frac{\partial v}{\partial r}+w\frac{\partial v}{\partial z}+\frac{vu}{r}=\nu\left[\frac{1}{r}\frac{\partial}{\partial r}\left(r\frac{\partial v}{\partial r}\right)-\frac{v}{r^2}\right], \tag{7}$$

$$u\frac{\partial w}{\partial r}+w\frac{\partial w}{\partial z}=-\frac{\partial(p/\rho)}{\partial z}+\nu\left[\frac{1}{r}\frac{\partial}{\partial r}\left(r\frac{\partial w}{\partial r}\right)\right], \tag{8}$$

where ν is the kinematic viscosity. The continuity equation (5) is automatically satisfied by using the stream function Ψ for the meridional motion:

$$w\equiv\frac{1}{r}\frac{\partial\Psi}{\partial r},\quad u\equiv-\frac{1}{r}\frac{\partial\Psi}{\partial z}. \tag{9}$$

We define the boundary layer variable of order one

$$\eta=r/\delta(z), \tag{10}$$

with $\delta/z\ll 1$. Because the matching conditions (1)–(3) involve simple power laws and there are no external characteristic lengths, the problem has a self-similar structure. Independently of the form of $\delta(z)$, the stream function within the thin viscous region must take the form

$$\Psi=\nu z f(\eta), \tag{11}$$

as follows from the standard boundary layer condition that the convective and viscous terms must be comparable, $w\sim\nu z/\delta^2$, and from the relation between Ψ and w, namely $w\sim\Psi/\delta^2$. The thickness δ of the boundary layer is determined by the particular form of the flow far from the viscous region, which may be written from equations (1) and (10) as

$$\eta\to\infty,\quad \Psi\to(W_o/m)\,r^m=(W_o/m)\,\delta^m\eta^m. \tag{12}$$

(Only the case $l=+1$ is considered because no solutions exist for $l=-1$, as shown in the Appendix.) Comparison between (11) and (12) yields

$$\delta(z)=(m\nu z/W_o)^{1/m}. \tag{13}$$

We now complete the definition of the boundary layer variables through

$$v=\frac{\nu z}{\delta^2}\gamma(\eta),\quad \frac{p}{\rho}=\frac{(\nu z)^2}{\delta^4}\beta(\eta). \tag{14}$$

such that the boundary conditions they satisfy at infinity involve pure numbers and powers of η:

$$\eta\to\infty,\quad f\to\eta^m,\quad \gamma\to\pm mL\eta^{m-2},\quad \beta\to\frac{(mL)^2}{2(m-2)}\eta^{2(m-2)}. \tag{15}$$

With these definitions, and using as independent variable $\xi \equiv \eta^2$, the boundary layer approximation to the Navier–Stokes equations becomes

$$\gamma^2 = 2\xi\beta. \tag{16}$$

$$2\frac{m-1}{m}\gamma f' - 2f\gamma' - \frac{f\gamma}{\xi} = 4\frac{\mathrm{d}}{\mathrm{d}\xi}(\xi\gamma') - \frac{\gamma}{\xi}, \tag{17}$$

$$\frac{2-m}{m}f'^2 + ff'' + \frac{1}{2m}[(2-m)\beta + \xi\beta'] = -2\frac{d}{d\xi}(\xi f'). \tag{18}$$

where primes denote differentiation with respect to ξ. The meridional velocity components are given by

$$w = \frac{\nu z}{\delta^2}2f', \quad u = -\frac{\nu}{r}\left(f - \frac{2\xi f'}{m}\right). \tag{19}$$

We shall look for solutions where p, w and v are finite at the axis. The second condition requires that f/ξ be finite at $\xi = 0$. Because (16) is singular at $\xi = 0$, γ^2/ξ must also be finite at $\xi = 0$. Accordingly, we will consider functions with the following behaviour as $\xi \to 0$:

$$f \sim \xi, \quad \gamma \sim \xi^{1/2}, \quad \beta \sim -1. \tag{20}$$

3. Solutions

To integrate numerically equations (16)–(18) one must know the behaviour of f, γ and β near the axis $\xi = 0$, and at infinity. The regularity conditions (20) require the following near-axis behaviour:

$$f = f_1\xi + f_2\xi^2 + f_3\xi^3 + \ldots, \tag{21}$$

$$\gamma = \xi^{1/2}(g_0 + g_1\xi + g_2\xi^2 + \ldots), \tag{22}$$

$$\beta = \beta_0 + \beta_1\xi + \beta_2\xi^2 + \ldots. \tag{23}$$

which substituted into equations (16)–(18) determines completely all the coefficients f_i, g_i and β_i in terms of the first three constants of the expansion f_1, g_0 and β_0. For the lower-order terms one finds

$$\beta_1 = g_0^2/2, \quad \beta_2 = g_0 g_1/2, \tag{24}$$

$$f_2 = \frac{m-2}{4m}\left(f_1^2 + \frac{\beta_0}{2}\right), \quad f_3 = \frac{1}{48m}[4(m-4)f_1 f_2 - (3-m)\beta_1]. \tag{25}$$

$$g_1 = -g_0 f_1/(4m). \tag{26}$$

Although there are three degrees of freedom to start the integration at $\xi = 0$, one of them is effectively irrelevant as a consequence of the fact that equations (16) (18) are invariant under the uniparametric group of transformations of scale

$$f \to f, \quad \xi \to C\xi, \quad \gamma \to \gamma/C, \quad \beta \to \beta/C^2. \tag{27}$$

Similarly, the coefficients entering in the power laws (15) for the boundary condition at $\xi \to \infty$ can be re-scaled, so that their absolute magnitude also becomes irrelevant. For convenience we choose C in (27) such that $\beta_0 = -1$, so that the initial and final conditions are, respectively,

$\xi \to 0$,

$$f = A_1\xi + \ldots, \quad \gamma = A_2\xi^{1/2} + \ldots, \quad \beta = -1 + \ldots; \tag{28}$$

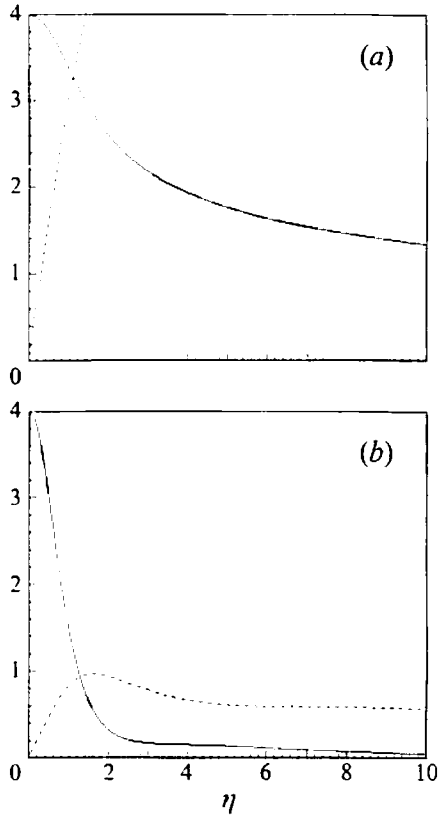

FIGURE 1. Velocity profile in the boundary layer for (*a*) $m = 8/5$ and (*b*) $m = 4/5$ ($A_1 = 2$). The continuous line represents $\delta^2 w/(\nu z) = f'(\eta)/\eta$; the dashed line, $ru/\nu = -\eta f'(\eta)/m + f(\eta)$ and the dotted line, $\delta^2 v/(\nu z) = \gamma(\eta)$. (See (14) and (19).)

$\xi \to \infty$.

$$f \to (C\xi)^{m/2}, \quad \gamma \to \pm B\xi^{(m-2)/2}, \quad \beta \to (B^2/[2(m-2)])\,\xi^{m-2}; \tag{29}$$

with

$$A_1 = f_1 C, \quad A_2 = g_0 C^{3/2}, \quad B = mLC^{m/2}. \tag{30}$$

Thus, starting at the origin with two degrees of freedom A_1 and A_2, one reaches the region $\xi \gg 1$ also with two degrees of freedom: C, determining the proper rescaling required in the solution found, and B, fixing the swirl parameter L arising at the Euler level. Linear analysis as $\xi \to \infty$ shows that the behaviour is

$$f \to (C\xi)^{m/2}[1 + P\xi^{\lambda_+} + Q\xi^{\lambda_-}], \tag{31}$$

where the exponents $\lambda_+ > \lambda_-$ are the roots of

$$\lambda^2 + (m-1)\lambda + m - 2 + (m-1)L^2/2 = 0, \tag{32}$$

both being real and of opposite signs for $0 < m < 2$. P and Q in (31) are free constants. The term proportional P dominates as $\xi \gg 1$, where Q is irrelevant. Accordingly, if one starts the numerical integration of equations (16)–(18) at $\xi = 0$ with behaviour (28), assigning arbitrary values to the two free constants A_1 and A_2, one will not encounter the desired behaviour $f = (C\xi)^{m/2}$ at infinity except for some exceptional trajectories for which the mode proportional to P is eliminated. As found by Long (1961) for the case $m = 1$, this circumstance requires picking up a certain value of $A_2(A_1)$ for each real A_1 in the interval $-1/\sqrt{2} < A_1 < \infty$. The behaviour is thus not drastically different in the whole range $0 < m < 2$ from that found by Long for $m = 1$. However, for $m = 1$ Long found that the swirl parameter L is always the

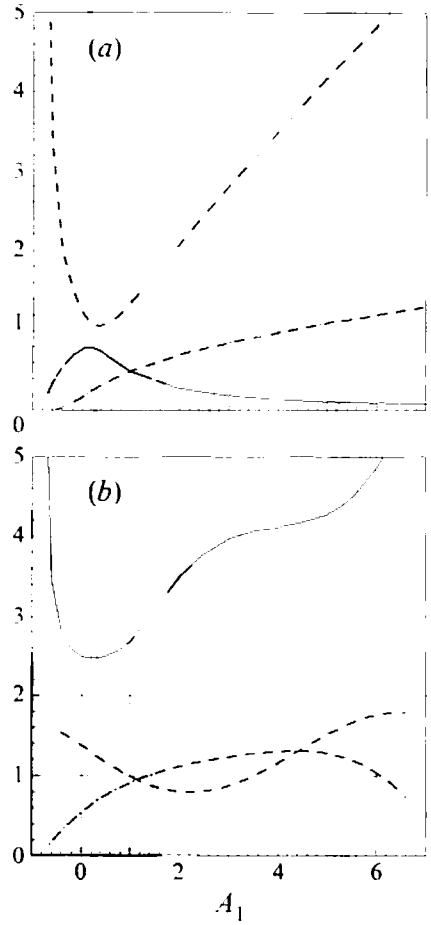

FIGURE 2. Values of A_2 (–.–.–), C^{m-2} (– – –) and L (– – –) as functions of A_1 for which solutions exist in the cases (*a*) $m = 8/5$ and (*b*) $m = 4/5$.

same, independently of the value of A_1. In fact, for $m = 1$ equation (18) becomes $f'^2 + ff'' + (\beta + \xi\beta')/2 = -2(\xi f')'$, which may be integrated once to

$$ff' + \beta\xi/2 + 2\xi f' = \text{constant}. \tag{33}$$

where the constant vanishes as a result of the boundary conditions at the origin. As $\xi \to \infty$ this first integral and (29)–(30) imply that

$$L = \sqrt{2} \quad (m = 1). \tag{34}$$

In other words, although the axial flow and the swirl entered with independent intensities at the Euler level through the two constants W_0 and L, somehow the condition of regularity at the origin kills this double freedom and couples the amount of circulation unequivocally to the axial flow through $L = \sqrt{2}$. When $m \neq 1$, there is no analogue to the integral (33) so that L is not uniquely fixed. However, we find numerically that equations (16)–(18) have solutions satisfying (28) and (29) only within a certain range of values of L which depends on m. This fact sometimes excludes swirlless flows.

Our numerical study has been based on Long's method which identifies $A_2(A_1)$ by shooting. Figures 1(*a*) and 1(*b*) show two examples of the boundary layer structures for $m = 8/5$, $A_1 = 2$, and $m = 4/5$, $A_1 = 2$, respectively. Figures 2(*a*) and 2(*b*) show the variation of the parameters A_2, C^{m-2} and L as functions of A_1 also for $m = 8/5$ and $m = 4/5$, respectively.

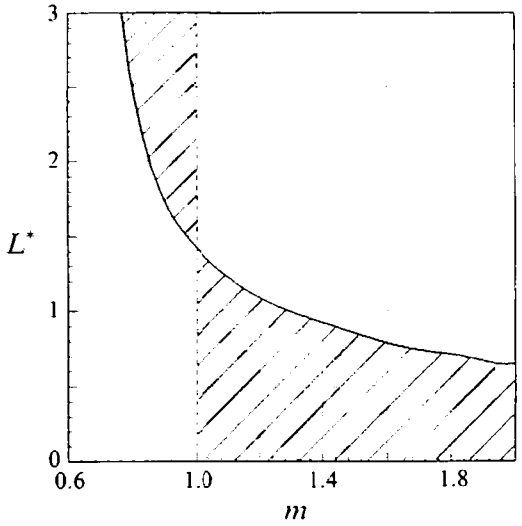

FIGURE 3. Regions of solution existence for the near-axis boundary layer in (L,m)-space (shaded areas), which is below the curve L^* for $m > 1$ and above it for $m < 1$. For $m = 1$ the only allowed value is $L = \sqrt{2}$.

The dashed area of figure 3 shows the region of solution existence in (L,m)-space, bounded between the vertical line $m = 1$ and a critical curve $L^*(m)$. For $m > 1$, solutions exist only below the curve, so that the swirl cannot exceed an m-dependent maximum value given by that curve. For $m < 1$, the domain of existence is above the curve, and the swirl must be larger than a minimum value. For $m = 1$, all solutions are characterized by $L = \sqrt{2}$. Therefore, flows with an arbitrarily small swirl are allowed only for $m > 1$, and flows involving mostly pure rotation may exist only for $m < 1$. These domains of solution existence are a consequence of the fact that $L(A_1)$ shows a maximum for $m > 1$ (e.g. figure 2*a*), a minimum for $m < 1$ (e.g. figure 2*b*), and takes a constant value ($L = \sqrt{2}$) for $m = 1$.

For the case $m = 1$, Long (1961) has provided a classification of the solutions based on the sign of the convective derivative of Bernoulli's function $H = p/\rho + u \cdot u/2$ along the axis. His analysis is straightforwardly generalized for all m in the range $0 < m < 2$. Thus, there are three types of solutions depending on whether A_1 belongs to one of the following intervals: $[-1/\sqrt{2}, 0]$, $[0, 1/\sqrt{2}]$ and $[1/\sqrt{2}, \infty]$ (see figure 4). In the first case w and u change sign in the vicinity of the axis so that there is a near-axis region where the fluid moves towards the apex; hence, the flow within the viscous boundary layer is divided into two cells. In the second case, the motion is everywhere away from the apex, but the maximum axial velocity is not located at the axis. In the third interval the flow represents a jet with the maximum axial velocity at the axis. The frontier values $A_1 = \pm 1/\sqrt{2}$ correspond to the zeros of f_2 in (25).

An alternative classification of Long's vortices ($m = 1$) was provided by Burggraf & Foster (1977) in relation to the *momentum transfer* or *flow force*

$$J \equiv 2\pi \int_0^\infty (p/\rho + w^2)\, r\, \mathrm{d}r,$$

which, as shown by Long (1961), is constant along the axis. In fact, for $m = 1$ and in our notation, the non-dimensional flow force M is given by

$$M \equiv \frac{J}{W_0^2 B^2} = \frac{\pi}{B^2} \int_0^\infty (\beta + 4f'^2)\, \mathrm{d}\xi \quad (m = 1) \tag{35}$$

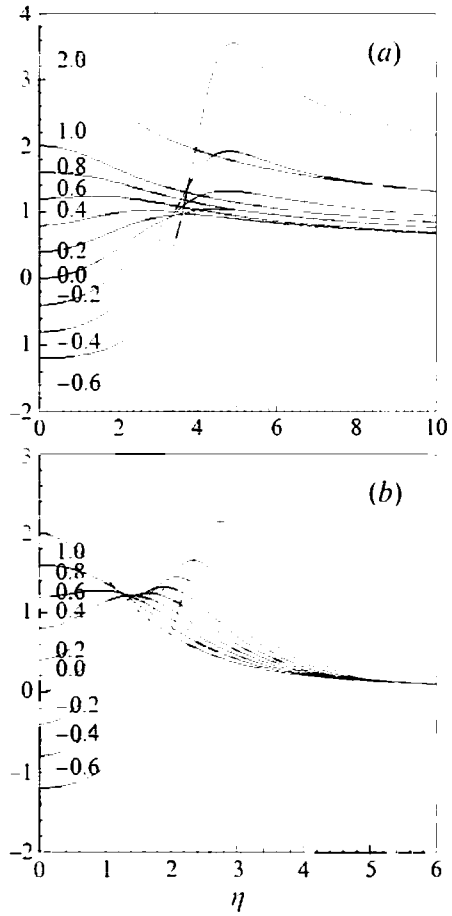

FIGURE 4. Axial velocity profiles, $\delta^2 w/(rz) = f'(\eta)/\eta$, for (*a*) $m = 8/5$ and (*b*) $m = 4/5$, and for several values of A_1, given on each curve. For $A_1 < 0$, the axial velocity is negative at the axis; for $0 < A_1 < 1/\sqrt{2}$, the axial velocity is positive at the axis, but its maximum is away from the axis; and for $A_1 > 1/\sqrt{2}$ the maximum is at the axis.

which does not depend on z (B is the scaling constant in (29)). M is a non-monotonic function of A_1, having a minimum $M = M^* \approx 3.75$ for $A_1 = A_1^* \approx 0.2$. Thus, for $M > M^*$, two possible vortices exist, while there is no solution for $M < M^*$. Since $A_1^* < 1/\sqrt{2}$, solutions with $A_1 < A_1^*$ (termed by Burggraf & Foster as type II solutions) have the maximum of the axial velocity w away from the axis, while solutions with $A_1 > A_1^*$ (type I) may have this maximum at the axis ($A_1 > 1/\sqrt{2}$), or away from it ($A_1^* < A_1 < 1/\sqrt{2}$). Burggraf & Foster showed that only the type II solutions are physically meaningful (see next section). For $m \neq 1$, the flow force M is not constant; but we have a similar situation with regard to the swirl parameter L, which, like the flow force for the case $m = 1$, does not depend on the axial coordinate. When $0 < m < 1$, two solutions exist for $L > L^*(m)$, and there is no solution for $L < L^*(m)$ (see figure 2*b* for the particular case $m = 4/5$); when $1 < m < 2$, no solutions exist for $L > L^*(m)$, and there are two possible solutions for $L < L^*(m)$ (figure 2*a*, $m = 8/5$). The value of $A_1^*(m)$ corresponding to $L^*(m)$ is found to be almost independent of m, being approximately equal to 0.1 for $0.9 < m < 1.5$. Following the classification of Burggraf & Foster, solutions for $A_1 > A_1^*$ and for $A_1 < A_1^*$ may be termed, respectively, as type I and type II solutions (see figure 5).

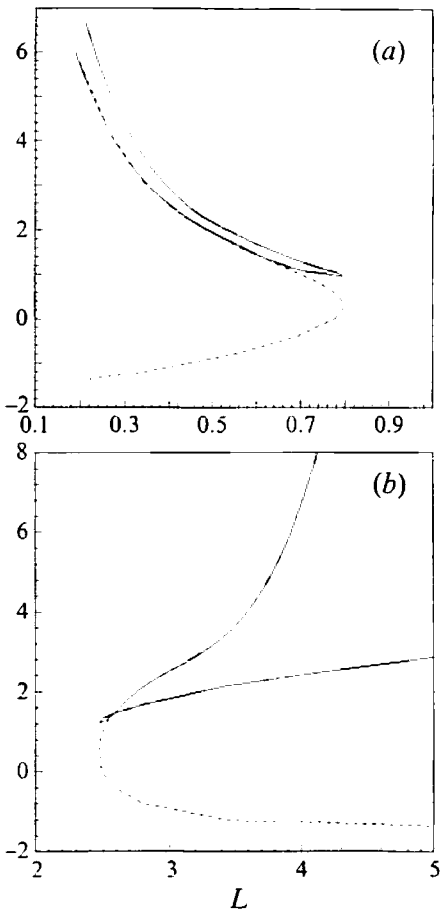

FIGURE 5. Maximum value of the axial velocity, $\delta^2 w/(\nu z)|_{max}$ (continuous lines), and axial velocity at the axis, $\delta^2 w/(\nu z)|_{\eta=0} = 2A_1$ (dashed lines), as functions of L for (*a*) $m = 8/5$ and (*b*) $m = 4/5$. In (*a*) there are two solutions for each value of $L < L^*(8/5) \approx 0.79$ ($A_1^*(8/5) \approx 0.15$); for (*b*), there are two solutions for $L > L^*(4/5) \approx 2.47$($A_1^*(4/5) \approx 0.28$). These solutions are termed as type I solutions for $A_1 > A_1^*$ (lower continuous curve and upper dashed curve in (*a*), and upper curves in (*b*)), and type II solutions for $A_1 < A_1^*$.

4. Discussion of the results and conclusions

The main conclusion of this study is that the axial singularities often appearing in axisymmetric inviscid swirling flows cannot always be regularized through thin viscous layers. As a result, a sharp boundary is established between some physically unacceptable inviscid flows and others whose existence is not forbidden by viscosity. For the axisymmetric inviscid flows considered, none with a near-axis motion directed towards the origin (and, therefore, away from the axis) may be regularized (see the Appendix for $l = -1$). A similar conclusion had already been reached for the special case $m = 1$ by Yih *et al.* (1982). For $l = 1$, the criterion for acceptability of the inviscid flow may be cast in terms of restrictions on the inviscid swirl parameter L, in qualitative analogy with real vortex flows (e.g. Spall *et al.* 1987), or in terms of the flow force M for the special case $m = 1$.

The fact that the solution of the near-axis boundary layer approximation to the Navier–Stokes equations for a family of vortices breaks down for values of a certain parameter above or below a threshold value supports the proposed explanation of the vortex breakdown phenomenon which relates it to boundary layer separation (Gartshore 1962 and Hall 1972, among others). According to this view, vortex

breakdown appears when the near-axis boundary layer equations governing approximately the viscous core of the vortex fail to have a solution. A complete picture of the phenomenon cannot be given just by a near-axis boundary layer approximation, because its solution breakdown may be a sufficient but not a necessary condition for vortex breakdown to occur (see, however, the work by Beran & Culik 1992 commented on below). However, we provide here a concrete clear-cut example which may illustrate this mathematical scenario for vortex breakdown. Actually, several among the main expectations from the theory are met in our example. For instance, there is indeed a drastic difference between those inviscid flows which are viable, and those with a slightly different value of L which are not; the transition is certainly of a catastrophic kind. Also, although the reasons leading to breakdown are strictly viscous, the resulting breakdown criterion in terms of the swirl parameter L (or M for $m = 1$) is independent of viscosity, in agreement with observations at high enough Reynolds numbers (see below). This result is a natural consequence of a boundary layer theory where viscosity is absorbed within an inner variable, becoming irrelevant for some matters (e.g. existence), while remaining relevant for others (e.g. stresses). Although this result was not mentioned explicitly in Hall's formulation, it was implicit from the analogous behaviour of the two-dimensional boundary layers. (For an example of when a similar inviscid criterion arises for strictly inviscid reasons, see Saffman's 1992 discussion of an older problem by Batchelor 1967.) The absence of viscosity from the matching conditions with the inviscid vortex is also manifest in equation (15).

4.1. *The special case $m = 1$*

As discussed above, the boundary layer solutions for the case $m = 1$ are qualitatively different from those corresponding to $m \neq 1$. For r^{-1} type vortices, Long's first integral (33) makes it evident that solutions exist only for $L = \sqrt{2}$. Solutions are appropriately classified in terms of the so-called flow force parameter M, (35): for M smaller than a critical value M^* (Long's value $M^* = 3.65$ was corrected by Burggraf & Foster 1977 to 3.75, in agreement with our results), no self-similar solutions exist; for $M > M^*$, two possible solutions exist, termed by Burggraf & Foster as type I and type II solutions. These authors also found a most interesting result. They sought numerical solutions to the near-axis boundary layer equations matching Long's inviscid asymptote, for given upstream conditions which did not necessarily coincide with the self-similar solution. When the value of the flow force M corresponding to their upstream condition (notice that M remains constant along the flow) was larger than the critical value M^*, they discovered that the boundary layer flow always evolved rapidly towards one of the two self-similar solutions (in particular to type II solutions; in later works, Foster & Duck 1982, Foster & Smith 1989, Foster & Jacqmin 1992), found that Long's vortex is unstable to small non-axisymmetric disturbances, but solutions of type II were more unstable than those of type I). But for $M < M^*$, when no self-similar solution exists, the viscous region readily invaded much of the flow field. Burggraf & Foster could thus conclude that lack of existence of self-similar solutions to the boundary layer equations for a certain conical outer vortex implied that the viscous core could not be confined to a narrow axial region. The outer vortex could accordingly not survive for long and would necessarily break down. Their study provides compelling evidence in favour of Hall's scenario associating vortex breakdown to the failure of the near-axis boundary layer equations.

These results were confirmed, extended and put into a wider perspective in recent works by Goldshtik & Shtern (1990) and by Shtern & Hussain (1993). These authors considered the conically similar solutions to the complete Navier-Stokes equations (i.e.

case $m = 1$; they used these solutions as a model tornado, as did Burggraf & Foster with Long's vortex). They found three branches of solutions forming a hysteresis loop with jump transitions between flow regimes. For high Reynolds numbers, two of these branches correspond, near the axis, to Long's solutions of type I and II, while the third (type III solutions) corresponds to a two-cell flow with a near-plane fan jet separating an inviscid, but rotational, outer cell from a potential flow inner cell. Interestingly enough, Shtern & Hussain (1993) find that, for decreasing M, a solution of type I jumps, when $M = M^*$, to a solution of type III with a two-cell flow structure. They have related this phenomenon to vortex breakdown, since the potential inner cell resembles the bubble structure with recirculating motion observed in some forms of vortex breakdown. They also find the opposite phenomenon, of abrupt vortex consolidation: for increasing M, when M reaches another critical value, a solution of type III jumps to a type I solution, so that a two-cell flow suddenly reorganizes itself into a near-axis swirling jet. The description given by Shtern & Hussain of the vortex breakdown phenomenon for r^{-1} type vortices supports Hall's analogy with boundary layer separation, though they believe that the failure of the near-axis boundary layer approximation is associated to a bistability phenomenon, which changes the global flow pattern, in close connection with the vortex breakdown theory of Leibovich (1978, 1984).

4.2. *The case* $m \neq 1$

For the wider class of flows with $0 < m < 2$ considered here, we have shown that only certain combinations of axial and azimuthal velocities are allowed, as mapped in figure 3. Nearly pure rotation is definitely forbidden for $m > 1$, where the region of solution existence corresponds to $0 < L < L^*(m)$, with $L^* < \sqrt{2}$. Nearly pure axial motion is impossible for $m \leqslant 1$.

For $m \neq 1$ the flow force is no longer constant along the vortex, but the swirl parameter L plays a role somewhat analogous to M for Long's vortices: when $0 < m < 1$, two self-similar solutions exist for $L > L^*(m)$, and there is no solution for $L < L^*(m)$; when $1 < m < 2$, no solutions exist for $L > L^*(m)$, and there are two possible solutions for $L < L^*(m)$ (see figures 2, 3 and 5). These results, in particular those for $1 < m < 2$, have a number of features in common with earlier numerical and experimental results for less idealized vortices.

For instance, based upon previous theoretical, numerical and experimental results, Spall *et al.* (1987) proposed a criterion for the onset of vortex breakdown in terms of a local Rossby number, which is equivalent to the inverse of our swirl parameter L. According to it, vortex breakdown occurs when L is above a critical value L^* which depends on the Reynolds number. For high Reynolds numbers, L^* tends to a constant approximately equal to 1.5, in qualitative agreement with our results for $1 < m < 2$. The agreement is quantitative (within experimental errors) for $m = 1^+[L^*(1^+) = \sqrt{2}]$.

More recently, Beran & Culik (1992) have solved numerically both the steady axisymmetric Navier–Stokes equations and their quasi-cylindrical approximation for swirling flows through pipes with a throat. They find that, for sufficiently large Reynolds numbers, vortex breakdown occurs abruptly above a critical value of the dimensionless vortex strength V (equivalent to our swirl parameter L) for the Burger vortex they use as the upstream boundary condition. For values of V (or L) above this threshold (which for high Reynolds numbers is always around 1.5), the solution of the near-axis boundary layer equations ceases to exist, jumping to another solution of the Navier–Stokes equations which models a typical bubble structure of vortex breakdown. Thus, the results of these authors also support Hall's theory on vortex breakdown. They are also in agreement with the more recent results of Shtern & Hussain for r^{-1} type

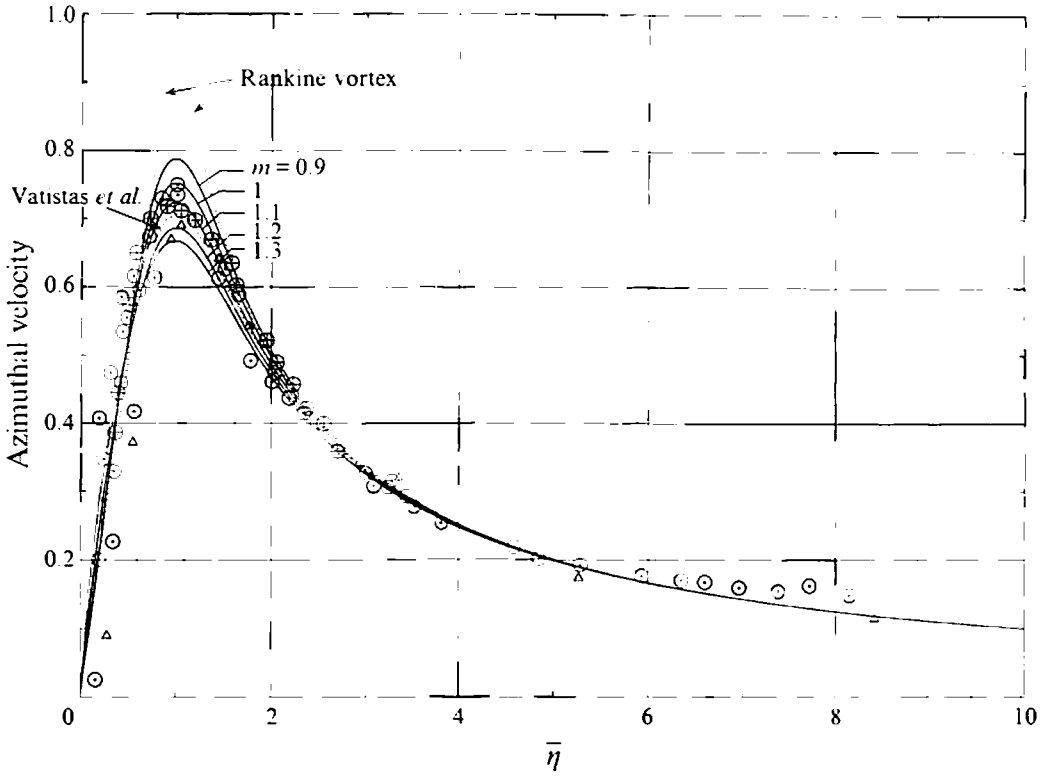

FIGURE 6. Comparison of experimental data by Vatistas *et al.* (1986) (⊙). Faler & Leibovich (1977) (⊕) and Robertson (1965) (△) with normalized azimuthal velocity profiles, $\bar{v}(\bar{\eta})$, for $m = 0.9$, 1, 1.1, 1.2 and 1.3 (continuous lines), all computed for $A_1 = A_1^*(m) \approx 0.1$. The upper dotted line corresponds to a Rankine vortex, and the lower one to an empirical model by Vatistas *et al.* (1991).

vortices, in the sense that there is a multiplicity of solutions of the Navier–Stokes equations, with sudden transitions (vortex breakdown) from a solution of the near-axis approximation to another one no longer modelled by this approximation. However, the parameter governing this transition in real flows is never the flow force of the r^{-1} type vortices, but is the swirl parameter L, in agreement with the criterion of Spall *et al.* and with the results of our model.

The theoretical work by Keller, Egli & Exley (1985) (see also Escudier 1988, and Wang & Rusak 1995) must also be mentioned here. These authors proposed a two-stage theory for vortex breakdown, in some ways similar to Benjamin's (1962) critical state theory, but with an initial isentropic transition, which accounts for the breakdown, before the non-isentropic one of the Benjamin's theory. They have studied analytically this isentropic transition for a Rankine vortex, finding that breakdown occurs above a critical value of a swirl parameter (equivalent to our parameter L) which depends on the Reynolds number. For high Reynolds numbers, this critical value tends exactly to $\sqrt{2}$, as in our results for $m = 1^-$.

The fact that the relevant breakdown parameter found in experiments and in numerical simulations of vortex flows is never the flow force M, but a swirl parameter L, seems to indicate that the inviscid vortex around most real vortex cores is not exactly irrotational ($m = 1$ or $v \sim r^{-1}$), but of the form $v \sim r^{-n}$, with power n in general smaller than one (m larger than one), as otherwise corroborated by many experimental data (see e.g. Ogawa 1993). Furthermore, the close agreement between the observed $L^* \approx 1.5$ for high Reynolds numbers and the model value $L^*(1^-) = \sqrt{2}$ is an indication that the experimental circumstances where vortex breakdown has been studied for high

Reynolds numbers would have been in some way described by a slightly perturbed r^{-1} type vortex. (Notice that our family of solutions shows that the case $m = 1$ is highly degenerate, since infinitesimal perturbations away from it lead from a region of existence with zero measure ($L = \sqrt{2}$), to a finite domain of existence $0 < L < \sqrt{2}$ for m slightly larger than 1 (figure 3).) To support this, figure 6 compares the azimuthal velocity profiles for some values of m of the family of self-similar vortex cores given here with experimental data for several high Reynolds numbers vortex cores just before vortex breakdown compiled by Vatistas, Lin & Kwok 1986. The theoretical curves also correspond to critical conditions $L = L^*(m)$, for which $A_1^*(m) \approx 0.1$. They have been normalized according to (36), which introduces no fitting parameter in the vertical scale:

$$\bar{v}(\bar{\eta}) \equiv \frac{2\pi\delta\eta_c v}{2\pi r(vz/\delta^2)B\eta^{m-2}} = \frac{\eta_c^{2-m}}{B}\frac{\gamma(\bar{\eta})}{\bar{\eta}^{m-1}}, \quad \bar{\eta} \equiv \frac{\eta}{\eta_c}, \tag{36}$$

where $\eta_c(m)$ is the position where $\gamma(\eta)$ has its maximum. The figure shows also the profile corresponding to the Rankine vortex, $\bar{v} = \bar{\eta}$ for $0 \leqslant \bar{\eta} \leqslant 1$ and $\bar{v} = 1/\bar{\eta}$ for $1 \leqslant \bar{\eta} < \infty$, and that of a simple model fitting the experimental data given by Vatistas *et al.* (1991), $\bar{v} = \bar{\eta}/(1+\bar{\eta}^4)^{1/2}$. The differences between the various curves are typically smaller than the scatter of the experimental data, except in the region near the maximum. There, most data points lie between our self-similar profiles corresponding to $m = 1$ and $m = 1.2$, while Vatistas' experimental model is between $m = 1.1$ and 1.2. It is thus clear that our model flow with m slightly larger than unity represents quite well not only the azimuthal velocity profile near breakdown, but also the critical value of L.

This work is dedicated to the memory of Professor Ignacio Da Riva, with whom two of the authors and former students (A. B. and J. F. M.) will always be in debt. It has been supported by the Dirección General de Investigación Científica y Tecnológica of Spain, PB90-1023 and PB93-0974, and by the US National Science Foundation Grant CTS-9319051.

Appendix

This paper has considered only the case $l = \pm 1$ in (1), when the inviscid flow in the vicinity of the axis moves upwards, with radial velocity towards the axis. No regularizing near-axis boundary layer solutions coupling to a member of the inviscid family considered exist in the opposite case when $l = -1$. To prove this consider the behaviour of the solution of (16)–(18) as $\xi \to \infty$. Introducing the functions

$$h = f\xi^{-m/2}, \quad k = \beta\xi^{2-m}, \quad s = \gamma\xi^{(2-m)/2}, \tag{A 1}$$

which tend to constants as $\xi \to \infty$, into the boundary layer equations (16)–(18), and linearizing around the far-field behaviour (29), one finds that $h'' \sim \exp[-l(C\xi)^{m/2}/m]$, with similar behaviour for k' and s'. Therefore, the modes associated with these higher-order derivatives decay exponentially at increasing ξ, provided that $l = 1$, which is the case analysed above. When $l = -1$, the behaviour is inverted and these modes grow at increasing ξ. Solutions cannot therefore exist when $l = -1$, as there are not enough available degrees of freedom to cancel all these divergences. Indeed, this can be shown explicitly for the case $m = 1$, for which equation (17) may be integrated once to

$$\frac{\mathrm{d}}{\mathrm{d}\xi}(\gamma\xi^{1/2}) = E\exp\left[-\int \mathrm{d}\xi \frac{f}{2\xi}\right], \tag{A 2}$$

where E is a free constant. For large ξ, f tends to $l(C\xi)^{1/2}$, so that the right-hand side of (A 2) grows exponentially without bound if $l = -1$. In order for γ to satisfy the boundary condition at ∞, it is thus essential that $E = 0$, in which case $\gamma\xi^{1/2}$ is constant throughout, and the boundary condition (28) at $\xi = 0$ cannot be met.

The impossibility of a boundary layer solution at the axis when the near-axis outer flow is directed away from the axis was reported by Yih *et al.* (1982) who considered conical viscous flow fields proportional to r^{-1} (case $m = 1$ in our notation), solving numerically the complete Navier–Stokes equations in that case. They also gave the physical explanation that, for that flow direction, there is no vorticity advection towards the axis to balance the outward viscous diffusion of vorticity away from the axis.

REFERENCES

BATCHELOR, G. K. 1964 Axial flow in trailing line vortices. *J. Fluid Mech.* 20, 645–658.

BATCHELOR, G. K. 1967 *An Introduction to Fluid Dynamics*, Section 7.5. Cambridge University Press.

BENJAMIN, T. B. 1962 Theory of the vortex breakdown phenomenon. *J. Fluid Mech.* 14, 593.

BERAN, P. S. & CULICK, F. E. C. 1992 The role of non-uniqueness in the development of vortex breakdown in tubes. *J. Fluid Mech.* 242, 491–527.

BOJAREVICS, V., FREIBERGS, YA., SHILOVA, E. I. & SHCHERBININ, E. V. 1989 *Electrically Induced Vortical Flows*, Chap. 2. Kluwer.

BUNTINE, J. D. & SAFFMAN, P. G. 1995 Inviscid swirling flows and vortex breakdown. *Proc. R. Soc. Lond.* A 449, 139–153.

BURGGRAF, O. R. & FOSTER, M. R. 1977 Continuation or breakdown in tornado-like vortices. *J. Fluid Mech.* 80, 685–703.

DRAZIN, P. G., BANKS, W. H. H. & ZATURSKA, M. B. 1995 The development of Long's vortex. *J. Fluid Mech.* 286, 359–377.

ESCUDIER, M. P. 1988 Vortex breakdown: observations and explanations. In *Prog. Aero. Sci.* 25, 189–229.

FALER, J. H. & LEIBOVICH, S. 1977 Disrupted states of vortex flow and vortex breakdown. *Phys. Fluids* 20 1385–1400.

FERNANDEZ-FERIA, R., FERNANDEZ DE LA MORA, J. & BARRERO, A. 1995 Conically similar swirling flows at high Reynolds numbers. Part 1. One-cell solutions. *SIAM J. Appl. Maths* (submitted).

FOSTER, M. R. & DUCK, P. W. 1982 The inviscid stability of Long's vortex. *Phys. Fluids* 25 1715–1718.

FOSTER, M. R. & JACQMIN, D. 1992 Non-parallel effects in the instability of Long's vortex. *J. Fluid Mech.* 244, 289–306.

FOSTER, M. R. & SMITH, F. T. 1989 Stability of Long's vortex at large flow force. *J. Fluid Mech.* 206, 405–432.

GARTSHORE, I. S. 1962 Recent work in swirling incompressible flow. *NRC Can. Aero. Rep.* LR-343.

GOLDSHTIK, M. A. 1960 A paradoxical solution of the Navier-Stokes equations. *Appl. Mat. Mech. (Sov.)* 24, 610–621.

GOLDSHTIK, M. A. & SHTERN, V. N. 1990 Collapse in conical viscous flows. *J. Fluid Mech.* 218, 483–508.

HALL, M. G. 1961 A theory for the core of a leading-edge vortex. *J. Fluid Mech.* 11, 209–228.

HALL, M. G. 1972 Vortex breakdown. *Ann. Rev. Fluid Mech.* 4, 195–218.

KELLER, J. J., EGLI, W. & EXLEY, J. 1985 Force and loss-free transitions between flow states. *Z. Angew. Math. Phys.* 36, 854–889.

KHORRAMI, M. R. & TRIVEDI, P. 1994 The viscous stability analysis of Long's vortex. *Phys. Fluids* 6, 2623–2630.

LANDAU, L. 1944 A new exact solution to the Navier-Stokes equations. *Dokl. Akad. Nauk SSSR* 43, 286–288.

LEIBOVICH, S. 1978 The structure of vortex breakdown. *Ann. Rev. Fluid Mech.* 10, 221–346.

LEIBOVICH, S. 1984 Vortex stability and breakdown: survey and extension. *AIAA J.* 22, 1192–1206.

LONG, R. L. 1958 Vortex motion in viscous fluid. *J. Met.* 15, 108–112.

LONG, R. L. 1961 A vortex in an infinite viscous fluid. *J. Fluid Mech.* 11, 611–625.

MAYER, E. W. & POWELL, K. G. 1992 Similarity solutions for viscous vortex cores, *J. Fluid Mech.* 238, 487–507.

OGAWA, A. 1993 *Vortex Flows*. CRC Press.

PAULL, R. & PILLOW, A. F. 1985*a* Conically similar viscous flows. Part 2. *J. Fluid Mech.* 155, 343–358.

PAULL, R. & PILLOW, A. F. 1985*b* Conically similar viscous flows. Part 3. *J. Fluid Mech.* 155, 359–379.

PILLOW, A. F. & PAULL, R. 1985 Conically similar viscous flows. Part 1. *J. Fluid Mech.* 155, 327–341.

ROBERTSON, J. M. 1965 *Hydrodynamics in Theory and Application*. Prentice-Hall.

SAFFMAN, P. G. 1992 *Vortex Dynamics*, Section 14.4. Cambridge University Press.

SHTERN, V. N. & HUSSAIN, F. 1993 Hysteresis in a swirling jet as a model tornado. *Phys Fluids* A 5, 2183–2195.

SOZOU, C. 1992 On solutions relating to conical vortices over a plane wall. *J. Fluid Mech.* 244, 633–644.

SOZOU, C., WILKINSON, L. C. & SHTERN, V. N. 1994 On conical flows in an infinite fluid. *J. Fluid Mech.* 276, 261–271.

SPALL, R. E., GATSKI, T. B. & GROSH, C. E. 1987 A criterion for vortex breakdown. *Phys. Fluids* 30, 3434–3440.

SQUIRE, H. B. 1951 The round laminar jet. *Q. J. Mech.* 4, 321–329.

SQUIRE, H. B. 1952 Some viscous fluid flow problems. 1. Jet emerging from a hole in a plane wall. *Phil. Mag.* 43, 942–945.

SQUIRE, H. B. 1956 Rotating fluids. In *Surveys in Mechanics* (ed. G. K. Batchelor & R. M. Davies). Cambridge University Press.

STEWARTSON, K. & HALL, M. G. 1963 The inner viscous solution for the core of a leading-edge vortex. *J. Fluid Mech.* 15, 306–318.

VATISTAS, G. H., KOZEL, V. & MIH, W. C. 1991 A simpler model for concentrated vortices. *Exps. Fluids* 11, 73–76.

VATISTAS, G. H., LIN, S. & KWOK, C. K. 1986 Theoretical and experimental studies on vortex chambers flows. *AIAA J.* 24, 635–642.

WANG, S. & RUSAK, Z. 1995 A theory of the axisymmetric vortex breakdown in a pipe. (Preprint.)

YIH, C. Y., WU, F., GARG, A. K. & LEIBOVICH, S. 1982 Conical vortices: a class of exact solutions of the Navier Stokes equations. *Phys. Fluids* 25, 2147–2157.